Heliyon 10 (2024) e28356

Contents lists available at ScienceDirect

Heliyon

journal homepage: www.cell.com/heliyon

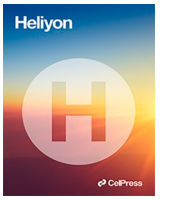

Research article

FAT1 upregulation is correlated with an immunosuppressive tumor microenvironment and predicts unfavorable outcome of immune checkpoint therapy in non-small cell lung cancer

Chao Chen [a,*], Yanling Li [b], Haozhen Liu [a], Mengying Liao [c], Jianyi Yang [a], Jixian Liu [a,**]

[a] *Department of Thoracic Surgery, Peking University Shenzhen Hospital, Shenzhen Peking University-The Hong Kong University of Science and Technology Medical Center, Shenzhen, 518035, China*
[b] *Central Laboratory, Peking University Shenzhen Hospital, Shenzhen, 518036, China*
[c] *Department of Pathology, Peking University Shenzhen Hospital, Shenzhen, 518035, China*

ARTICLE INFO

Keywords:
FAT1
SERPINE1
Immune checkpoint inhibitors
Non-small cell lung cancer
Tumor microenvironment

ABSTRACT

Background: Previous studies found that *FAT1* was recurrently mutated and aberrantly expressed in multiple cancers, and the loss function of *FAT1* promoted the formation of cancer-initiating cells in several cancers. However, in some types of cancer, *FAT1* upregulation could lead to epithelial-mesenchymal transition (EMT). The role of *FAT1* in cancer progression, which appears to be cancer-type-specific, is largely unknown.

Methods: QRT-PCR and immunochemistry were used to verify the expression of *FAT1* in non-small cell lung cancer (NSCLC). QRT-PCR and Western blot were used to detect the influence of siFAT1 knockdown on the expression of potential targets of *FAT1* in NSCLC cell lines. GEPIA, KM-plotter, CAMOIP, and ROC-Plotter were used to evaluate the association between *FAT1* and clinical outcomes based on expression and clinical data from TCGA and immune checkpoint inhibitors (ICI) treated cohorts.

Results: We found that *FAT1* upregulation was associated with the activation of TGF-β and EMT signaling pathways in NSCLC. Patients with a high *FAT1* expression level tend to have a poor prognosis and hard to benefit from ICI therapy. Genes involved in TGF-β/EMT signaling pathways (*SERPINE1, TGFB1/2,* and *POSTN*) were downregulated upon knockdown of *FAT1*. Genomic and immunologic analysis showed that high cancer-associated fibroblast (CAF) abundance, decreased $CD8^+$ T cells infiltration, and low TMB/TNB were correlated with the upregulation of *FAT1*, thus promoting an immunosuppressive tumor microenvironment (TME) which influence the effect of ICI-therapy.

Conclusion: Our findings revealed the pattern of *FAT1* upregulation in the TME of patients with NSCLC, and demonstrated its utility as a biomarker for unfavorable clinical outcomes, thereby providing a potential therapeutic target for NSCLC treatment.

* Corresponding author.
** Corresponding author.
E-mail addresses: gkd.chaochen@foxmail.com (C. Chen), 252110465@qq.com (J. Liu).

https://doi.org/10.1016/j.heliyon.2024.e28356
Received 29 October 2023; Received in revised form 17 March 2024; Accepted 17 March 2024
Available online 22 March 2024

1. Introduction

FAT atypical cadherin 1 (*FAT1*) encodes a transmembrane protein involved in cell proliferation, adhesion, and migration [1]. Recent studies have shown that *FAT1* was frequently mutated in multiple cancers [2]. The loss function of *FAT1* leads to the activation of MAPK/ERK signaling, Hippo, and Wnt/β-catenin signaling pathways which are involved in the development of several cancers [3–7]. For example, *FAT1* mutations and deletions are associated with tumor progression in melanoma, head and neck squamous cell carcinoma (HNSCC), esophageal squamous cell carcinoma (ESCC), and oral cancer, suggesting a tumor suppressor role in these cancers [3–5]. However, it should be noted that *FAT1* has been found to promote tumor progression in breast cancer (BRCA), colorectal cancer (CRC), hepatocellular carcinoma (HCC), cervical cancer (CESC), and glioma [6,7]. For instance, *FAT1* is involved in regulating the production of inflammatory cytokines, promoting glioma progression [7,8]. These studies suggest that *FAT1* may exhibit different or even opposite functions in a cancer-specific manner.

Over the past decade, immunotherapy technologies, particularly immune checkpoint inhibitors (ICI), have made substantial progress in treating cancer [9–12]. To screen patients with the potential benefits of ICI therapy, many studies have been devoted to finding molecular markers in response to ICI therapy [12–14]. Several genomic markers were found to be associated with ICI efficacy, such as PD-L1, mismatch repair defects (dMMR), tumor mutation burden (TMB), and tumor neoantigen burden (TNB) [15–17]. However, these molecular markers still cannot fully explain the mechanism of ICI response. For example, patients with PD-L1 positive or TMB-high still failed to benefit from ICI therapy [18,19]. Thus, it was urgent to elucidate the response mechanism and molecular markers of ICI treatment [20]. Wenjing Zhang and colleagues found that *FAT1* mutant melanoma/NSCLC patients could be sensitive to ICI therapy [21]. Immunogenicity analysis suggested that *FAT1* mutant tumors had a higher TMB and immune cell infiltration [21].

In addition to PD-L1, MSI, and TMB, the tumor microenvironment (TME) is also associated with ICI response. An important determinant of the response to ICI is the presence of $CD8^+$ T cells in the TME [22,23]. In addition, the aggregation of cancer-associated fibroblasts (CAFs) in tumor nests can prevent the infiltration of T cells, thus affecting the prognosis of immunotherapy [24,25]. Interestingly, Khushboo Irshad discovered that *FAT1* can stimulate the expression of *TGFB1/TGFB2* and the formation of an immunosuppressive TME in glioma [26]. This indicates that the upregulation of *FAT1* may play a role in TME regulation, potentially affecting the effectiveness of immunotherapy.

Here, we found that *FAT1* upregulation was associated with an immunosuppressive TME via promoting the secretion of proteins in the TGF-β/EMT signaling pathway in non-small cell lung cancer (NSCLC). The upregulation of *FAT1* was associated with poor prognosis of NSCLC and can affect the ICI therapy efficacy. In immunogenicity analyses and in vitro experiments, *FAT1* was associated with an increase in CAF abundance and reduced infiltration of $CD8^+$ T cells. Our results indicate that *FAT1* may have a role in promoting immunosuppressive microenvironments via activating TGF-β/EMT signaling in NSCLC, which may also extend to other cancer types.

2. Materials and methods

2.1. Samples and data collection

The expression matrix for lung adenocarcinoma (LUAD) and lung squamous cell carcinoma (LUSC) in TCGA was downloaded from the UCSC Xena database (https://toil-xena-hub.s3.us-east-1.amazonaws.com/download/tcga_RSEM_gene_tpm.gz). Based on the tumor type, the TPM expression matrix was extracted from 509 LUAD and 479 LUSC samples.

In the study, BEAS-2B, a human normal lung epithelial cell line, and four lung adenocarcinoma cell lines (A549, H1299, H838, H1975) were obtained from the American Type Culture Collection (ATCC) and used for in vitro validation.

2.2. Differentially expressed genes (DEGs) analysis

The comparison of the expression level of *FAT1* between tumor and normal samples of the TCGA cohort was conducted using the GEPIA2 tool (http://gepia2.cancer-pku.cn) which used the expression data from the UCSC Xena database. The samples with expressions higher than the median value in the LUAD (255 samples) or LUSC (240 samples) cohort were defined as the FAT1-high subgroups. The limma package (version 3.52.3) was used to detect the DEGs between the FAT1-high subgroup and the FAT1-low subgroup in LUAD and LUSC. The parameter 'decide Tests DGE (adjust.method = "fdr", p.value = 0.01, lfc = 0.25)' was used to identify the DEGs. The visualization was performed using ggplot2 (version 3.3.6).

2.3. GSEA enrichment analysis of DEGs

The TPM expression matrix of LUAD (509 samples) and LUSC (479 samples) was used for GSEA enrichment analysis. For GSEA analysis in LUAD, 255 samples in the FAT1-high subgroup were compared to 254 samples in the FAT1-low subgroup; for GSEA analysis in LUSC, 240 samples in the FAT1-high subgroup were compared to 239 samples in the FAT1-low subgroup. 'h.all.v2022.1.Hs.symbols.gmt' were used as gene sets database when running enrichment tests.

2.4. Quantitative RT-PCR (qRT-PCR)

The expression of *FAT1* was detected using the Absolute Blue qRT-PCR SYBR green mix, following the manufacturer's instructions.

The comparative Ct method was used to examine double-stranded DNA-specific expression with $2^{-\triangle\triangle Ct}$. Primers used for *FAT1* were forward: 5′ AAAATAGGTGAAGAGACAGGTGT 3′ and reverse: 5′ TCTGTGGTGCATTGTCATTGA 3'.

2.5. RNA interference

Short interfering RNAs (siRNAs) for human *FAT1* (FAT1 Stealth siRNA #HSS103568) and the siRNA negative control (Stealth RNAi™ siRNA Negative Control Med GC Duplex #3 Cat #12935113) were purchased from ThermoFisher. Cells were transfected with siRNA using Lipofectamine 3000 and collected for further experiments 72 h after transfection.

2.6. Immunochemistry (IHC)

Formalin-fixed paraffin-embedded (FFPE) tumors and paired normal tissues were retrospectively collected from 10 NSCLC patients at the Department of Thoracic Surgery, Peking University Shenzhen Hospital. In this study, all patients provided informed consent prior to participation. Immunohistochemistry staining was performed following the previously described protocol [20]. The immunostaining scores of FAT1 were assessed in five randomly selected regions of each sample using a scoring system that considers staining intensity (0 = none, 1 = weak, 2 = moderate, 3 = strong) and positivity percentage (0 = 0–5%, 1 = 6–25%, 2 = 26–50%, 3 = 51–75%, 4 = 76–100%). The two values were multiplied to obtain a final score. The final score ranged from 0 to 12.

2.7. Western blot

Cell samples were lysed with cold RIPA lytic buffer (PL001-2A). The extracted protein was quantified using the Pierce BCA Protein Assay Kit (ThermoFisher, #23228). After electrophoresis on a sodium dodecyl sulfate-polyacrylamide gel (SDS-PAGE), the blots were transferred to a polyvinylidene difluoride (PVDF) membrane and incubated with 3% bovine serum albumin (BSA) for 2 h. The membranes were incubated with diluted primary antibodies FAT1 (#0905-4, 1:5000, HuaBio), SERPINE1 (A19096, 1:1000, ABclonal), NOX4 (A3656, 1:1000, ABclonal), and periostin (HPA012306, 1:500, Sigma) at 4 °C overnight, then the second antibody was added and incubated for 1 h at room temperature. The protein bands were detected on a chemiluminescence instrument.

2.8. Survival analysis

Several online databases, including the GEPIA2 (http://gepia2.cancer-pku.cn), KM-plotter (http://kmplot.com/analysis/index.php?p=service), CAMOIP (https://www.camoip.net), and ROC-Plotter (https://www.rocplot.org) were used to explore the prognostic value of *FAT1* expression in human cancers [27–29]. The expression value in the GEPIA2 database was collected from the TCGA cohort. We used GEPIA2 to investigate the correlations between the expression of *FAT1* and the overall survival (OS) and the disease-free survival (DFS) in LUAD and LUSC. In the GEPIA2 database, the median *FAT1* expression was used as a cutoff value to classify FAT1-hign and FAT1-low subgroups. KM-plotter was used to explore the prognostic value of *FAT1* in the ICI-treated cohorts. The prognostic difference between the FAT1-high and FAT1-low subgroups was calculated using the 'Auto select best cutoff' option. ROC-Plotter was used to compare *FAT1* expression between responders and non-responders.

2.9. Acquisition of TMB and TNB

The mutation data of the TCGA NSCLC cohort was downloaded from the Genomic Data Commons (GDC) database (https://gdc.cancer.gov/about-data/publications/pancanatlas). TMB was defined as the number of non-silent mutations (missense, nonsense, indel, splice-site) per sample in the TCGA NSCLC cohort. TNB was defined as the number of neoantigens per sample in The Cancer Immunome Atlas (TCIA) database (https://www.tcia.at/home).

2.10. The correlation between FAT1 and CAFs/CD8$^+$ T cells abundance

The Tumor Immune Estimation Resource (TIMER2.0) database (http://timer.cistrome.org) was used to evaluate the correlation between *FAT1* expression level and the abundance of CAFs and CD8$^+$ T cells in the TCGA cohort. TIMER2.0 provides a gene module that allows users to interactively explore the associations between TME composition (immune infiltrates, CAF abundance, etc.) and genetic (gene expression, etc.) or clinical features.

2.11. Statistical analysis

Statistical analyses were conducted using RStudio (version 2022.07.1) and R software (version 4.2.1). The correlation between *FAT1* and other genes was calculated using the 'cor.test' function with Spearman's method. A significance level of $P < 0.05$ was used, unless otherwise specified.

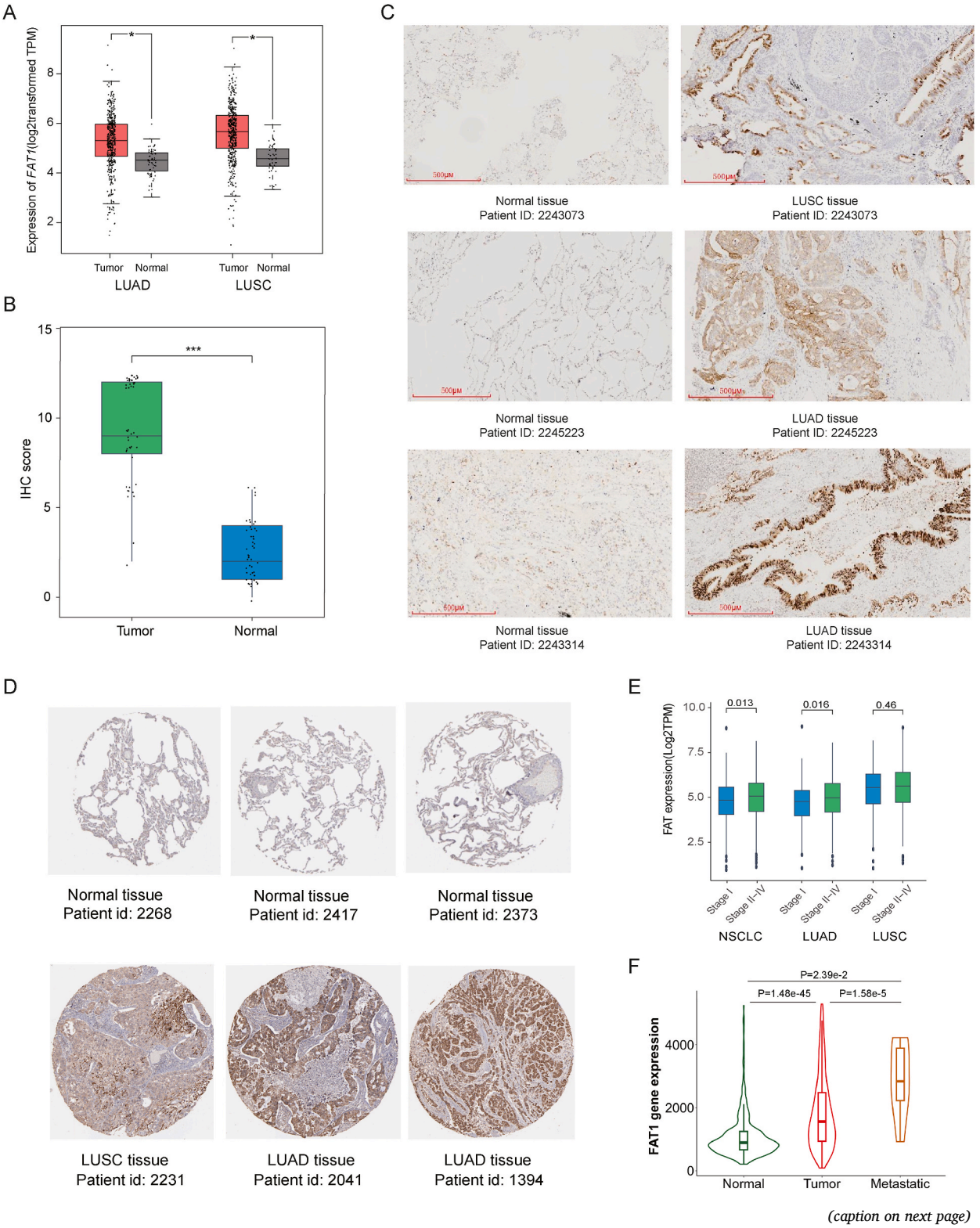

(caption on next page)

Fig. 1. Expression of *FAT1* in NSCLC. A. *FAT1* was upregulated in tumor samples compared to normal samples in LUAD and LUSC of the TCGA cohort. B. IHC score of FAT1 between tumor and normal samples from patients with NSCLC. C. Representative IHC images showed higher FAT1 protein level expression in tumors than in paired normal samples. D. The protein level expression of FAT1 in tumors compared to normal samples in the Human Protein Altas (HPA) database. Normal samples have a low protein level expression (top), while tumor samples have a high protein level expression (below), three normal samples and tumor samples were selected from the HPA database. E. *FAT1* was differentially expressed between early-stage tumor samples (stage I) and advanced-stage tumor samples (stage II-IV). F. *FAT1* was differentially expressed between normal, tumor, and metastatic samples in lung cancer using the online web tool: https://tnmplot.com/analysis, the 'gene chip data' was selected for analysis. *, $P < 0.05$, ***, $P < 0.001$, Wilcoxon rank sum test.

3. Results

3.1. In vitro validation of FAT1 expression in NSCLC

We initially compared the expression of *FAT1* in tumor and normal samples from the TCGA cohort using GEPIA2. Results showed that the expression of *FAT1* was significantly higher in the tumor samples compared to the normal samples in both LUAD and LUSC ($P < 0.05$, Fig. 1A). We further validated the expression of *FAT1* using IHC in ten tumors and paired normal samples from patients with NSCLC. FAT1 protein levels were higher in tumor samples compared to normal samples (Fig. 1B–C). In the Human Protein Atlas (HPA) database, the protein level of FAT1 was also found to be higher in tumors than in normal samples (Fig. 1D). Furthermore, according to the HPA database, *FAT1* expression was predominantly observed in epithelial cells, alveolar cells, smooth muscle cells, and fibroblasts, with minimal expression in other cell types in lung tissues (Supplementary Fig. 1). Furthermore, by analyzing the *FAT1* expression and copy number alterations (CNAs) in the TCGA database, we found that the upregulation of *FAT1* was associated with copy number gains in LUAD, and there was no significant association between copy number gain/amplification with *FAT1* expression in LUSC (Supplementary Fig. 2), indicating the existence of other mechanisms.

Interestingly, when comparing the expression of *FAT1* between different tumor stages in the TCGA NSCLC cohort, it was found that *FAT1* expression was higher in advanced tumors (stage II-IV) compared to early-stage tumors (stage I). This suggests a potential association between *FAT1* and tumor progression in NSCLC, particularly in patients with LUAD ($P = 0.016$; Wilcoxon rank sum test, Fig. 1E). Furthermore, we utilized TNMplot (https://tnmplot.com/analysis/) to compare the expression of *FAT1* in normal, tumor, and metastatic lung tissues. The results indicate that *FAT1* expression is higher in metastatic tissue than in primary tumor tissue and normal tissue (Fig. 1F), providing further evidence of the association between *FAT1* and the progression and metastasis of lung cancer.

3.2. High expression of FAT1 was associated with a poorer prognosis for NSCLC patients

We further investigated the relationship between *FAT1* expression and the prognosis of NSCLC using the GEPIA2 database. It was found that high *FAT1* expression (expressions higher than the median value) was significantly associated with unfavorable disease-free survival (DFS) of LUAD ($P = 0.014$, $HR = 1.8$; Fig. 2A) and LUSC ($P = 0.015$, $HR = 1.9$; Fig. 2B). Similarly, high *FAT1* expression was associated with unfavorable overall survival (OS) of NSCLC (Fig. 2D–E), especially in LUAD ($P = 0.0023$, $HR = 1.9$; Fig. 2D). If we consider LUAD and LUSC together as NSCLC, the *FAT1* expression was negatively associated with OS and DFS of patients with NSCLC ($P = 0.0061$, $HR = 1.6$; $P = 0.00045$, $HR = 1.6$, separately; Fig. 2C–F). Furthermore, multivariate Cox regression analysis showed that *FAT1* was an independent risk of OS for patients with LUAD ($P = 0.04$, $HR = 1.413$; Fig. 2G–H). The same trend was observed in LUSC, although not significant ($P = 0.128$, $HR = 1.23$; Supplementary Fig. 3). A nomogram prognostic model was constructed for LUAD using statistically significant factors from the multivariate Cox regression analysis. Based on the multivariate Cox analysis, these variables were assigned to the nomogram model. The number of points for each variable was determined using a straight line, and then recalibrated within the range of 0–100. The locations of the variables were calculated and recorded as the overall score. The probability of patients with LUAD surviving 1, 3, and 5 years can be determined by drawing vertical lines from the total-point axis down to the outcome axis (Supplementary Fig. 4).

3.3. High FAT1 expression was associated with the activation of TGF-β and EMT signaling

Since *FAT1* is highly expressed in NSCLC, we aimed to identify the genes and pathways associated with its upregulation. To achieve this, we downloaded expression data for LUAD ($N = 509$) and LUSC ($N = 479$) from the UCSC Xena database. The LUAD and LUSC cohorts were divided into FAT1-high and FAT1-low subgroups based on the median expression of *FAT1* in each cohort, separately. The limma method was used to identify DEGs between the FAT1-high and FAT1-low subgroups (Fig. 3A–B). In LUAD, the FAT1-high subgroup had 1475 up-regulated and 2314 down-regulated genes (Fig. 3C–Supplementary Table S1). Interestingly, many collagen-coding genes were upregulated, such as *COL1A1*, *COL1A2*, *COL3A1*, *COL4A1*, *COL10A1*, *COL11A1*, and *COL17A1*. In addition, several CAF-related genes were upregulated in the FAT1-high group, such as *POSTN*, *INHBA*, *NOX4*, and *THBS2* (Fig. 3A). On the other hand, several T cell marker genes (such as *CD3D, CD3E, CD8A, CD69*) and lots of MHC molecules (*HLA-E, CD74, HLA-DOA, HLA-DOB, HLA-DPA, HLA-DRA* et al.) were found to be downregulated (Fig. 3A). In LUSC, there were 1393 up-regulated and 2886 downregulated genes (Fig. 3C–Supplementary Table S2). Similarly, collagen-coding genes, such as *COL1A1, COL1A2, COL5A1, COL5A2,* and *COL11A1*, as well as CAF-related genes, such as *TGFB1*, *NOX4*, *POSTN*, *INHBA*, and *THBS2*, were up-regulated. Several T cell marker genes (*CD3E, CD3G, CD8A, CD8B, CD69* et al.) and many MHC molecules (*HLA-C, HLA-E, HLA-G, HLA-DOA, HLA-DMB* et al.) were downregulated in the FAT1-high subgroup (Fig. 3B).

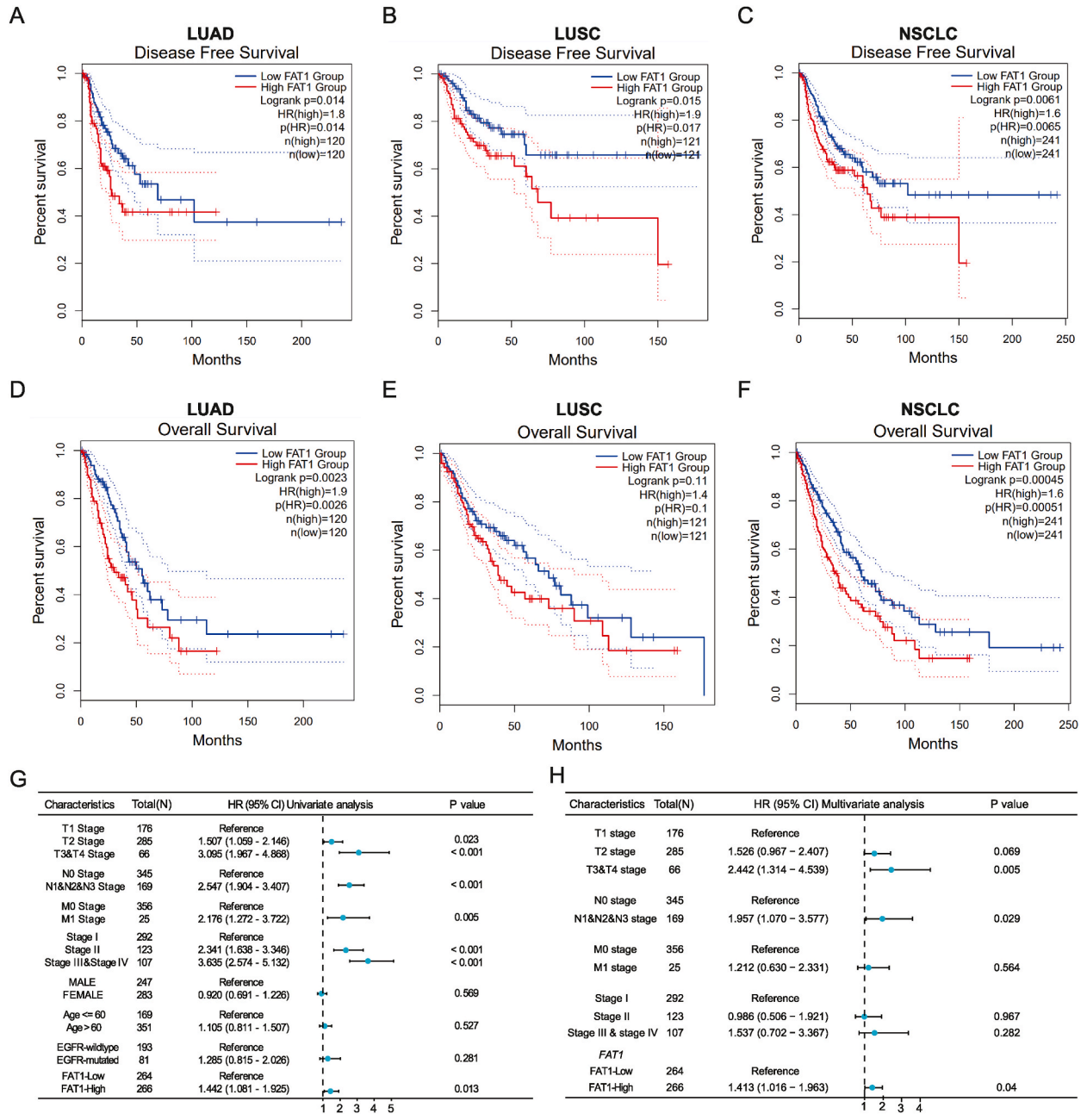

Fig. 2. *FAT1* was associated with the prognosis of patients with NSCLC. A-C. The difference in progression-free survival (PFS) compared between patients with LUAD (A), LUSC (B), and NSCLC (C) in FAT1-high and FAT1-low subgroups of the TCGA cohort. D-F. The difference in overall survival (OS) compared between patients with LUAD (D), LUSC (E), and NSCLC (F) in FAT1-high and FAT1-low subgroups of the TCGA cohort. The median expression of *FAT1* across samples in TCGA-LUAD cohort, TCGA-LUSC cohort, and TCGA-NSCLC cohort was defined as the cutoff value for each cohort. G-H. Univariate (G) and multivariate (H) Cox regression analysis between *FAT1* expression level and prognosis of LUAD with age, gender, TNM stage, EGFR mutation, and smoking considered. In multivariate analysis, only variables with a P value less than 0.05 in univariate Cox regression were considered. Blue box: hazard ratio (HR); black scale bar, 95% confidence interval of HR.

When comparing the DEGs between LUAD and LUSC cohorts, 1760 DEGs overlapped (Fig. 3D), consisting of 46.7% and 41.1% DEGs of LUAD and LUSC, separately. We performed functional enrichment analysis using GSEA to further investigate the function of these DEGs [30]. As expected, the TGF-β signaling pathway, epithelial-mesenchymal-transition (EMT), and hallmark_G2M_Checkpoint were found to be activated in the FAT1-high subgroup both in LUAD and LUSC (all with FDR<0.05, Fig. 3E–F). These findings suggest that *FAT1* may play a role in regulating the generation of CAFs and the progression/metastasis of NSCLC.

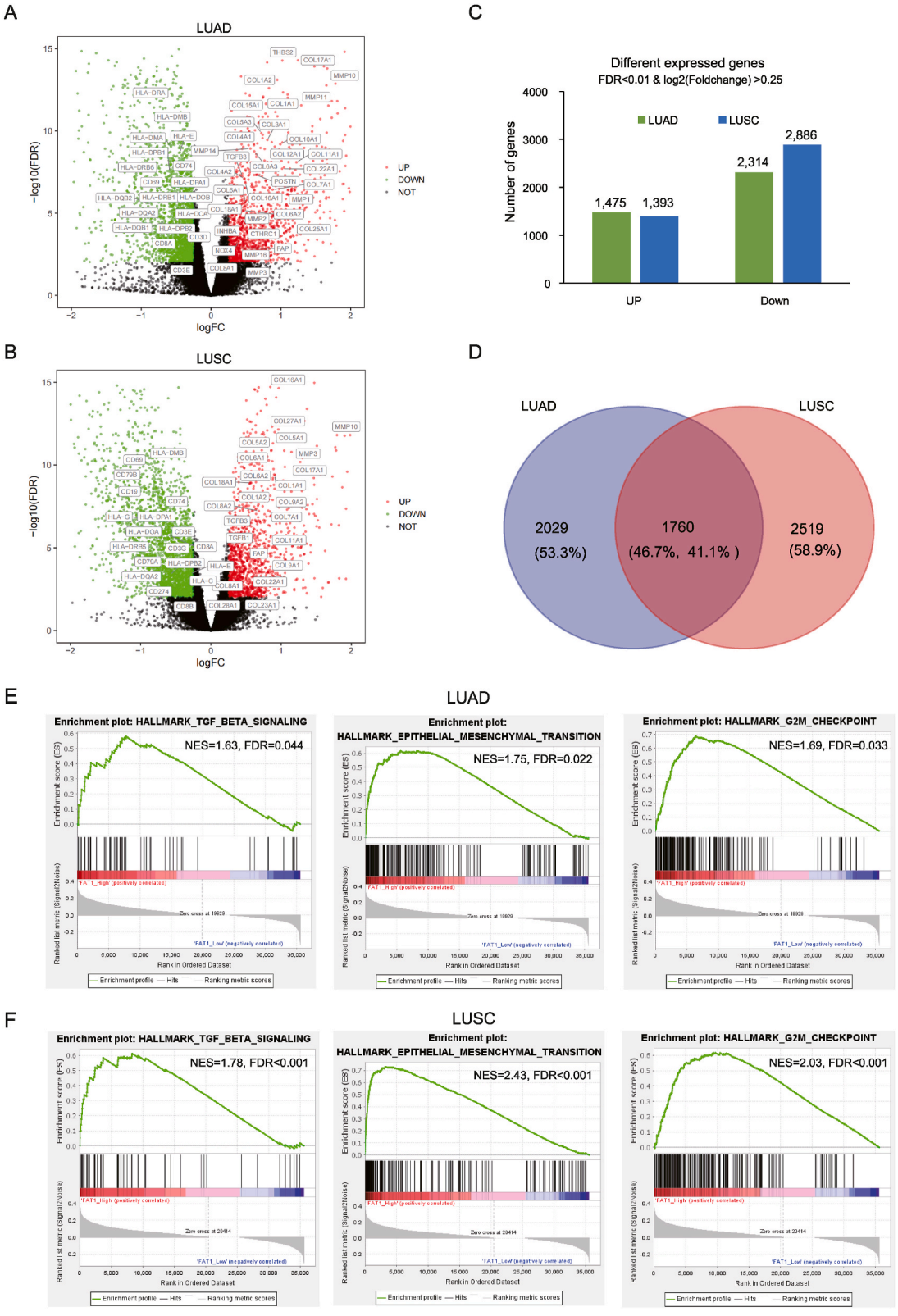

(caption on next page)

Fig. 3. Differential expressed genes (DEGs) and functional enrichment analysis between FAT1-high and FAT1-low subgroups in NSCLC. A. The volcano plot of DEGs between *FAT1*-high and *FAT1*-low samples in LUAD. B. The volcano plot of DEGs between *FAT1*-high and *FAT1*-low samples in LUSC. C. DEGs number in LUAD and LUSC samples. D. the Venn plot of the DEGs between LUAD and LUSC. E-F. The representative significantly enriched pathways of DEGs in LUAD (E) and LUSC (F) between *FAT1*-high and *FAT1*-low subgroups.

3.4. Knockdown of FAT1 leads to decreased expression of SERPINE1

It has been reported that *FAT1* can regulate genes involved in the TGF-β signaling pathway, such as *TGFβ1/2* and *SERPINE1*, in glioblastoma [26]. To investigate the potential targets of *FAT1* in lung cancer, we conducted in vitro knockdown experiments. We first explored the expression of *FAT1* in four LUAD cell lines using qRT-PCR and Western blot. *FAT1* was found to be significantly upregulated in mRNA and protein levels in two cell lines (A549 and H1299, $P < 0.05$; Fig. 4A–B). Then, we investigated the impact of *FAT1* knockdown on the expression of genes involved in TGF-β signaling, including *TGFB1, TGFB2, SERPINE1*, and *POSTN*. Interestingly, it was discovered that these genes were downregulated in both the A549 and H1299 cell lines after the knockdown of *FAT1* (Fig. 4C–D).

We further investigated whether knockdown of *FAT1* affects the secretion levels of proteins involved in the TGF-β signaling pathway, including Serpine1, Periostin, TGF-β1, and NOX4. It was found that TGF-β1, Serpine1, NOX4, and Periostin reduced in A549 cell lines after *FAT1* knockdown (Fig. 4E), Serpine1 and NOX4 were also reduced in H1299 cell lines after *FAT1* knockdown (Fig. 4E). Notably, *SERPINE1* is a member of the TGF-β signaling pathway and plays important roles in the regulation of EMT and metastasis in several cancers [31,32]. By conducting survival analysis using the GEPIA2 tool (http://gepia2.cancer-pku.cn), we found that a high expression level of *SERPINE1 (*the expression higher than the median value across samples*)* was associated with unfavorable survival of patients with LUAD or LUSC (Fig. 4F–G).

3.5. High FAT1 expression was correlated with increased CAF abundance and decreased $CD8^+$ T cell infiltration in NSCLC

As *FAT1* upregulation was associated with the activation of TGF-β and EMT signaling, and *FAT1* upregulation could influence the expression of *SERPINE1* and *NOX4*, we hypothesized that *FAT1* upregulation might influence the formation of CAFs in NSCLC. Immunologic analyses were conducted to investigate the potential influence of *FAT1* elevation. In both LUAD and LUSC, we observed a significant correlation between the expression level of *FAT1* and the abundance of CAF (Fig. 5A–B). In addition, *FAT1* was positively correlated with multiple CAF-related genes and collagen-coding genes in LUAD and LUSC, such as *POSTN*, *NOX4*, *SERPINE1*, *THBS2*, *COL1A1*, *COL1A2*, *COL4A1* and *COL11A1* (Supplementary Fig. 7). Interestingly, it was found that *FAT1* expression was negatively correlated with the abundance of $CD8^+$ T cells in both LUAD and LUSC, as determined by various methods (EPIC, MCPCOUNTER, and QUENTISEQ, all with $R < -0.1$ and $P < 0.01$; Fig. 5C–D). CIBERSORT algorithm further confirmed decreased $CD8^+$ T cells abundance in the FAT1-high subgroups in LUAD and LUSC compared to FAT1-low subgroups (both $P < 0.05$; Fig. 5E–F), indicating a negative factor for ICI therapy [14,33]. Finally, we want to know the potential association of *FAT1* with CAF composition and $CD8^+$ T cells in other cancer types. Consistently, a significant correlation between *FAT1* expression level and CAF abundance was observed in multiple cancers, such as adrenocortical cancer (ACC), BRCA, CESC, and diffuse large B-cell lymphoma (DLBC) (Supplementary Fig. 8A). In addition, the CAF marker genes, including *COL1A1*, *COL11A1*, *POSTN*, *NOX4*, and *THBS2*, were consistently positively correlated with *FAT1* (Supplementary Fig. 8B), while $CD8^+$ T cell marker genes were negatively correlated with *FAT1* (Supplementary Fig. 8B). The data indicate that *FAT1* expression is linked to increased CAF levels and reduced infiltration of $CD8^+$ T cells in various types of cancer.

Interestingly, we also found that the expression of *FAT1* was associated with decreased TMB and TNB in patients with LUAD ($R = -0.17$, $P = 0.00012$, and $R = -0.16$, $P = 0.00059$, respectively; Supplementary Figs. 9A–B), indicating its association with tumor immunogenicity. Similar results were detected in the LUSC cohort ($R = -0.11$, $P = 0.016$, and $R = -0.12$, $P = 0.1$, respectively; Supplementary Figs. 9C–D).

3.6. FAT1 upregulation was correlated with unfavorable clinical outcomes of ICI therapy in patients with NSCLC

Considering the potential roles of *FAT1* in regulating TME and tumor immunogenicity, we investigated the correlation between *FAT1* upregulation and clinical outcomes in patients treated with ICI. Our analysis of the CAMOIP database revealed a negative association between *FAT1* expression and the effectiveness of ICI treatment in NSCLC (HR = 2.36, 95% CI 0.97–5.75, P = 0.041; Fig. 6A). When considering age and gender, the high expression of *FAT1* remains an independent predictor for the benefit of ICI therapy (HR = 3.05, 95% CI 1.15–8.06, P = 0.025; Fig. 6B).

Furthermore, *FAT1* was also associated with worse prognosis in ICI-treated patients with several other tumor types, such as glioma (HR = 3.57, 95% CI 1.04–12.33; P = 0.032; Fig. 6C), urothelial cancer (HR = 1.65, 95% CI 1.2–2.28; P = 0.0021; Fig. 6D), and bladder cancer (HR = 1.74, 95% CI 0.94–3.21; P = 0.074; Fig. 6E). In addition, KM-plotter [27] analysis showed that patients in FAT1-high subgroups had a shorter OS compared to the FAT1-low group (HR = 1.6, 95% CI 1.35–1.9, P < 3.9e-8; Fig. 6F) in 933 pan-cancer patients treated with ICI. ROC-Plotter [29] analysis consistently showed that *FAT1* expression was significantly higher in non-responders compared to responders (P = 0.038, Fig. 6G).

Finally, we want to know which drugs can affect FAT1 expression. Comparative Toxicogenomics Database (CTD, http://ctdbase.org) was used to establish a FAT1-drug interaction network, illustrating the impact of various anticancer drugs on *FAT1* expression. The interaction network was visualized using Cytoscape (ver.3.8.2). The findings indicate that several drugs (cyclosporine, temozolomide, etc.) can potentially influence the expression of *FAT1* (Supplementary Fig. 10).

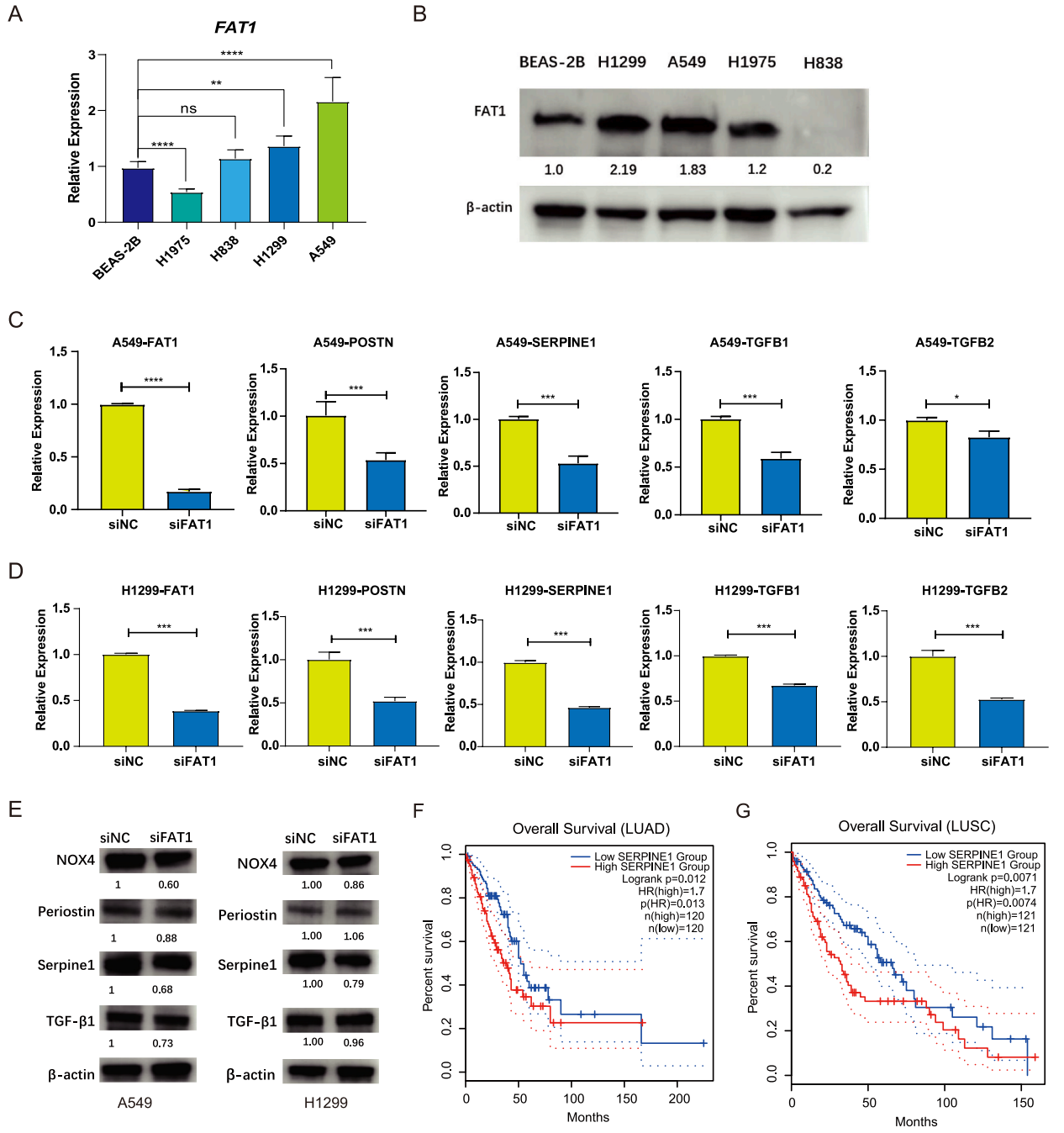

Fig. 4. Knockdown of *FAT1* inhibits the expression of TGF-β/EMT-related genes in NSCLC cell lines. A. *FAT1* was upregulated in two NSCLC cell lines (H1299 and A549) compared to normal cell lines BEAS-2B. B. The protein expression level of FAT1 in NSCLC cell lines compared to BEAS-2B, full-length gels and blots were shown in Supplementary Fig. 5. C-D. The expression of *POSTN*, *SERPINE1*, *TGFB1*, and *TGFB2* after knockdown of *FAT1* in A549 (C) and H1299 (D) cell lines. E. Western blot showed the influence of *FAT1* knockdown on the secretion of TGF-β/EMT-related proteins (NOX4, Periostin, Serpine1, and TGF-β1), full-length gels and blots were shown in Supplementary Fig. 6. F-G. The difference in OS compared between patients with LUAD (F), and LUSC (G) in SERPINE1-high and SERPINE1-low subgroups of the TCGA cohort. The samples with expressions higher than the median value in the TCGA cohort were defined as the SERPINE1-high subgroups. Data were shown as the mean ± SD (n = 3). *p < 0.05, **P < 0.01, ***P < 0.001, ****P < 0.0001.

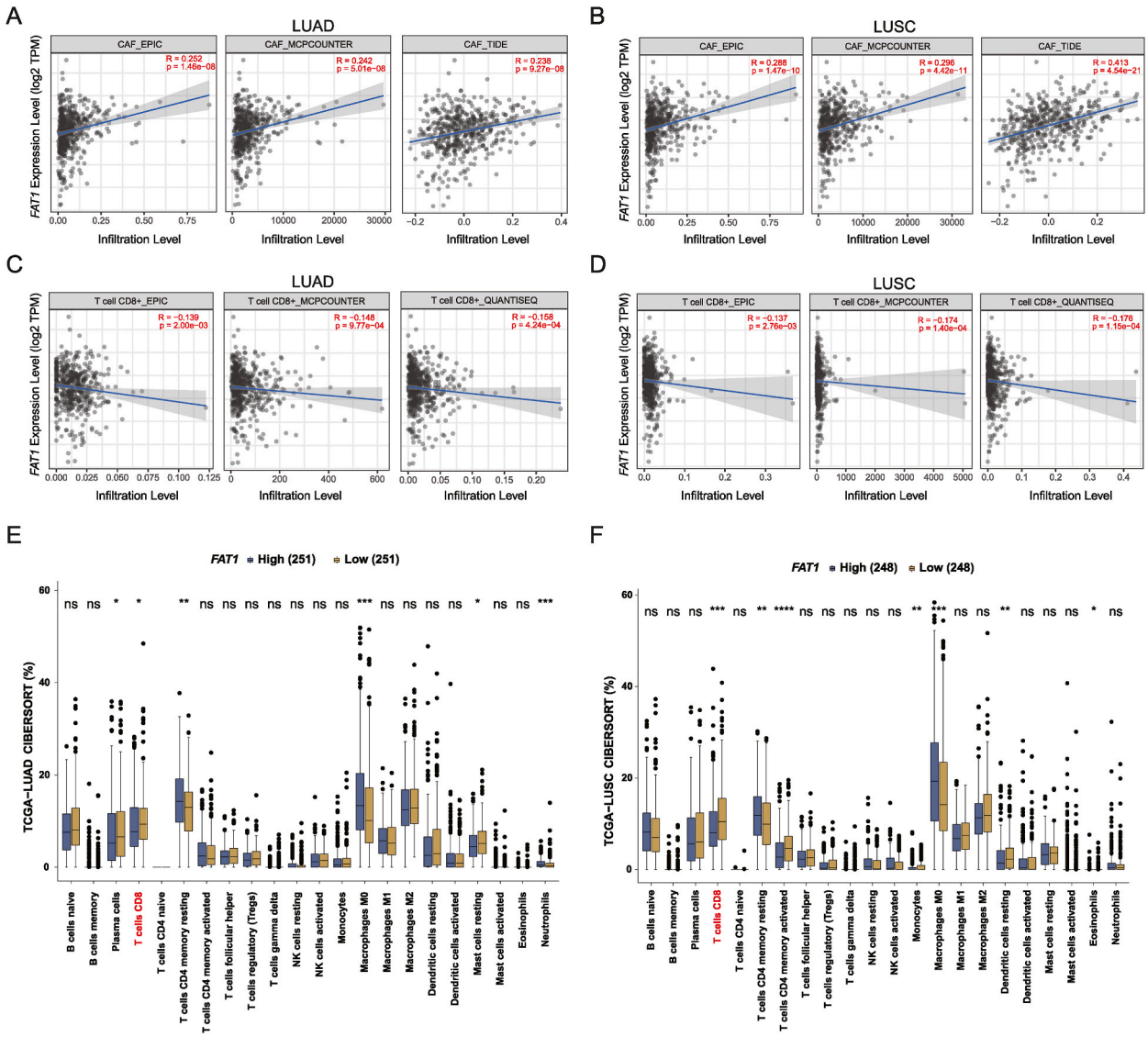

Fig. 5. Immunologic analyses between *FAT1*-high and *FAT1*-low subgroups in NSCLC. The significant positive correlation between *FAT1* expression and abundance of CAFs was confirmed in LUAD (A) and LUSC (B) by three different methods (EPIC, MCPCOUNTER, and TIDE). The significant negative correlation of *FAT1* expression and abundance of $CD8^+$ T cells was confirmed in LUAD (C) and LUSC (D) by three different methods (EPIC, MCPCOUNTER, and QUANTISEQ). The abundance of immune infiltration cells in LUAD (E) and LUSC (F) was calculated with CIBERSORT, separately. Significantly differentially infiltrated $CD8^+$ T cells between two subgroups were highlighted with red. The abundance of cell proportions in A-D was estimated by TIMER2.0 (http://timer.cistrome.org).

4. Discussions and conclusion

The role of *FAT1* in the development of tumors remains under investigation. At present, it is believed that *FAT1* may act either as a tumor suppressor or as a tumor oncogene, according to the type of cancer [1,34]. In HNSCC [5], ESCC [35], BRCA [36,37], and cervical cancer [38], *FAT1* expression was downregulated, which promotes the activation of MAPK/ERK signaling pathway and Hippo and Wnt/β-catenin signaling pathways. On the other hand, *FAT1* expression was upregulated in gastric cancer [39], glioma [7], and HCC [40], which promotes tumor proliferation, migration, invasion, and EMT. However, the large size of the *FAT1* coding sequence (13, 767bp) imposed significant restrictions on molecular manipulation, resulting in limited understanding of *FAT1*. Many questions are still unanswered, such as the upstream signals of *FAT1*, the molecular mechanism of how *FAT1* is dysregulated, and whether *FAT1* is an adhesion molecule or a signaling protein.

In NSCLC, it was found that the deletion of *FAT1* led to the transformation of the hybrid EMT phenotype in mouse models of LUSC, the hybrid EMT phenotype had also been observed in human LUSC [4]. Furthermore, cutaneous squamous cell carcinoma cells knocked out for *FAT1* showed resistance to both afatinib (an EGFR inhibitor) and trametinib (a MEK inhibitor) [4]. Therefore, the

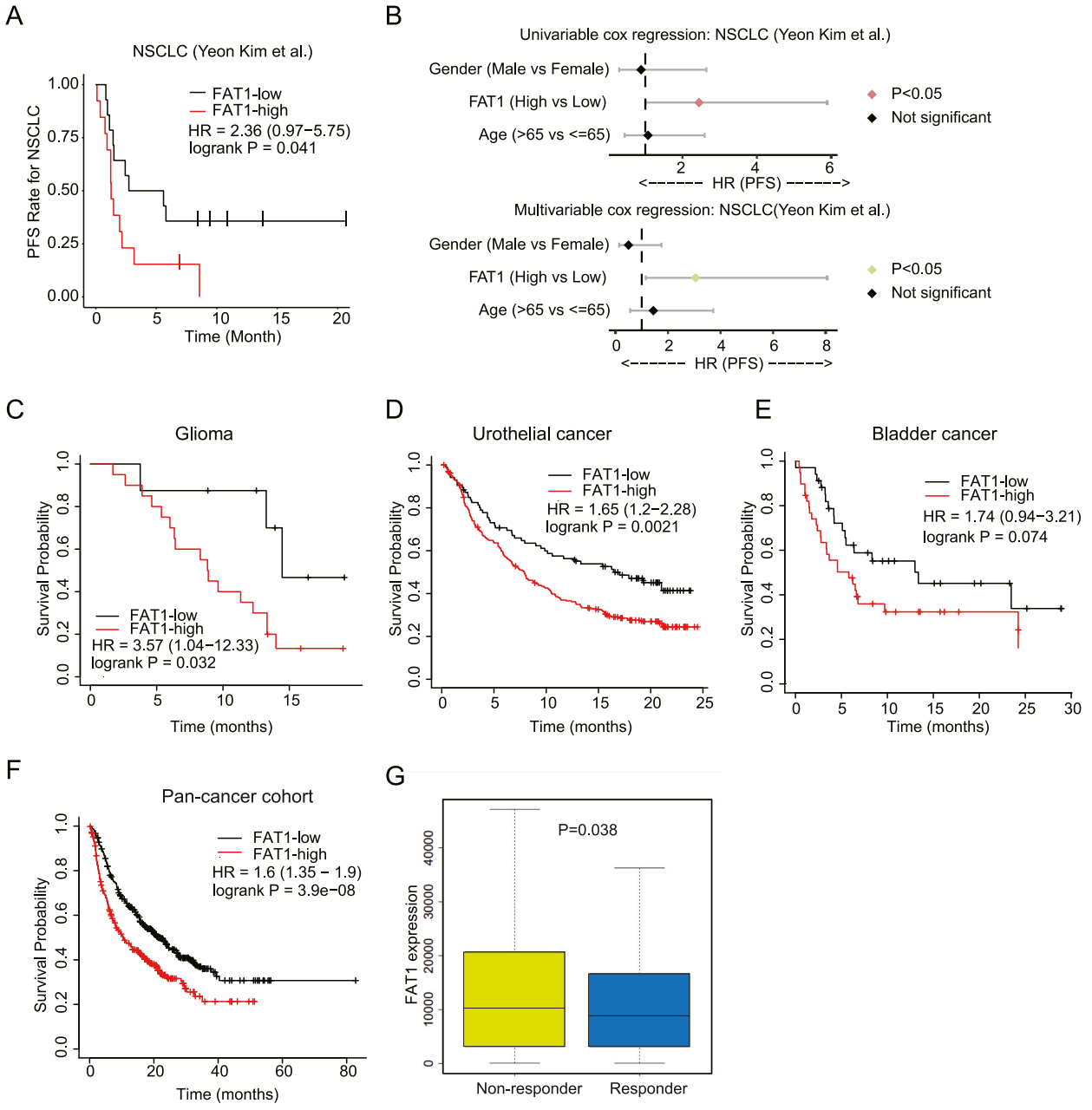

Fig. 6. *FAT1* expression was associated with a worse prognosis in cancer patients who received ICI therapy. A. Patients in the FAT1-high subgroup (higher than the median value across samples) have an unfavorable clinical outcome compared to the FAT1-low subgroup in the NSCLC cohort (N = 27, Yeon Kim et al.) who received ICI therapy. B. High *FAT1* expression was an independent risk factor for NSCLC patients who received ICI therapy. Univariable and multivariable Cox regression models between *FAT1* expression and prognosis of NSCLC were performed. C-E. High *FAT1* expression was associated with unfavorable clinical outcomes in patients with glioma (C, HR = 3.57, 95% CI 1.04–12.33, P = 0.032), urothelial cancer (D, HR = 1.65, 95% CI 1.2–2.28, P = 0.0021), and bladder cancer (E, HR = 1.74, 95% CI 0.94–3.21, P = 0.074). F. High *FAT1* expression was associated with unfavorable clinical outcomes in pan-cancer patients (HR = 1.6, 95% CI 1.35–1.9, P = 3.9e-8). G. Patients have a higher expression of *FAT1* in the non-responder subgroup than the responder subgroup who received ICI therapy (Mann-Whitney test, P = 0.038). KM-plotter was used to explore the prognostic value of *FAT1* expression in human cancers that received ICI therapy. ROC-Plotter (https://www.rocplot.org) was used to compare the *FAT1* expression between patients in responder and non-responder subgroups.

identification of the role of *FAT1* in EMT could have a significant impact on the treatment of cancer. Interestingly, we observed the upregulation of *FAT1* expression in patients with LUAD and LUSC. Additionally, we also found that the upregulation of *FAT1* may promote the progression of NSCLC through the activation of TGF-β and EMT signaling pathway (Figs. 3 and 4), which was consistent with those in hepatocellular carcinoma and glioma [26,40]. These results indicate that loss of function (deletion or mutation) and

overexpression of *FAT1* may both contribute to tumor progression, so it was required to maintain an equilibrium of *FAT1* function *in vivo*.

The tumor immune microenvironment was critical to the efficacy of ICI therapy [22,41–44]. Wenjing Zhang et al. found that patients with melanoma and NSCLC carrying *FAT1* mutations were more likely to benefit from ICI therapy [21]. In addition, the *FAT1* variant was associated with higher TMB and proinflammatory immune cell (e.g., activated $CD4^+$/$CD8^+$ T cells, M1 macrophages) infiltration, suggesting that *FAT1* may be involved in the regulation of the TME. Khushboo Irshad et al. found that the upregulation of *FAT1* could lead to the formation of a suppressive immune microenvironment by promoting the TGF-β signaling pathway [26]. In this study, we found that *FAT1* upregulation was associated with CAF abundance in NSCLC. In addition, a significant negative correlation of *FAT1* expression with $CD8^+$ T cell abundance was observed through digital cytometry [45]. Previous studies have shown that $CD8^+$ T cell infiltration could predict the effect of ICI [46], while CAFs can prevent the infiltration of T cells and thus prevent the curative effect of ICI therapy [25,47,48]. Collectively, we speculate that the up-regulation of *FAT1* promotes the formation of CAFs through elevation of TGF-β signaling and then blocks the infiltration of T cells, thus forming a suppressive TME that was not conducive to ICI treatment.

There are a few limitations in our study that need to be taken into considerations. Firstly, this work provided a detailed in silico analysis of the correlation between *FAT1* expression and high CAF, reduced $CD8^+$ infiltration, and low TMB/TNB, whereas the mechanism needs to be clarified in experiments in subsequent studies. Secondly, we verified the correlation between *FAT1* expression and TGF-β/EMT signaling genes (*SERPINE1*, *TGFB*1/2, and *POSTN*), however, the gene interaction network also remains to be explored in future.

In summary, we found that the upregulation of *FAT1* was associated with the activation of TGF-β/EMT pathways. Furthermore, high *FAT1* expression was found to be associated with increased CAF abundance, decreased $CD8^+$ T cells infiltration, and low TMB/TNB, thus promoting an immunosuppressive TME, which influence the efficiency of ICI-therapy. Therefore, continuing to study *FAT1* may be critical in helping to predict and treat NSCLC patients.

Ethics approval and consent to participate

Not applicable.

Funding

This research is supported by the Basic and Applied Basic Research Foundation of Guangdong Province under Grant No. 2022A1515111138.

Data availability statement

The clinical information and expression data of the TCGA cohort and ICI-treated cohorts in this study were collected from the cBioPortal database (https://www.cbioportal.org) and UCSC Xena database (https://xenabrowser.net/datapages/), other supporting information can be found in the supplementary files.

CRediT authorship contribution statement

Chao Chen: Writing – original draft, Visualization, Methodology, Data curation. **Yanling Li:** Validation, Methodology. **Haozhen Liu:** Methodology, Data curation. **Mengying Liao:** Methodology. **Jianyi Yang:** Writing – review & editing. **Jixian Liu:** Supervision, Resources, Project administration.

Declaration of competing interest

The authors declare that they have no known competing financial interests or personal relationships that could have appeared to influence the work reported in this paper.

Acknowledgments

We sincerely thank Dr. Dehua Lu, Ying Li, and Yun Wu for their suggestion for this work. We would also like to thank Duolaimi Biotechnology (Wuhan) Co., Ltd. for their experimental support in qRT-PCR.

Abbreviations

ICI	Immune checkpoint inhibitor
HR	Hazard ratio
NSCLC	Non-small cell lung cancer
LUAD	Lung adenocarcinoma
LUSC:	Lung squamous cell carcinoma

HNSCC	Head and neck squamous cell carcinoma
BRCA	Breast cancer
CRC	Colorectal cancer
ESCC	Esophageal squamous cell carcinoma

Appendix A. Supplementary data

Supplementary data to this article can be found online at https://doi.org/10.1016/j.heliyon.2024.e28356.

References

[1] Z. Peng, Y. Gong, X. Liang, Role of FAT1 in health and disease, Oncol. Lett. 21 (5) (2021) 398.
[2] L.G. Morris, A.M. Kaufman, Y. Gong, et al., Recurrent somatic mutation of FAT1 in multiple human cancers leads to aberrant Wnt activation, Nat. Genet. 45 (3) (2013) 253–261.
[3] K. Nakaya, H.D. Yamagata, N. Arita, et al., Identification of homozygous deletions of tumor suppressor gene FAT in oral cancer using CGH-array, Oncogene 26 (36) (2007) 5300–5308.
[4] I. Pastushenko, F. Mauri, Y. Song, et al., Fat1 deletion promotes hybrid EMT state, tumour stemness and metastasis, Nature 589 (7842) (2021) 448–455.
[5] S.C. Lin, L.H. Lin, S.Y. Yu, et al., FAT1 somatic mutations in head and neck carcinoma are associated with tumor progression and survival, Carcinogenesis 39 (11) (2018) 1320–1330.
[6] P. Meng, Y.F. Zhang, W. Zhang, et al., Identification of the atypical cadherin FAT1 as a novel glypican-3 interacting protein in liver cancer cells, Sci. Rep. 11 (1) (2021) 40.
[7] B. Dikshit, K. Irshad, E. Madan, et al., FAT1 acts as an upstream regulator of oncogenic and inflammatory pathways, via PDCD4, in glioma cells, Oncogene 32 (33) (2013) 3798–3808.
[8] E. Madan, B. Dikshit, S.H. Gowda, et al., FAT1 is a novel upstream regulator of HIF1α and invasion of high grade glioma, Int. J. Cancer 139 (11) (2016) 2570–2582.
[9] J. Tang, J.X. Yu, V.M. Hubbard-Lucey, et al., The clinical trial landscape for PD1/PDL1 immune checkpoint inhibitors, Nat. Rev. Drug Discov. 17 (12) (2018) 854–855.
[10] Suzanne L. Topalian, G. Drake Charles, M. Pardoll Drew, Immune checkpoint blockade: a common denominator approach to cancer therapy, Cancer Cell 27 (4) (2015) 450–461.
[11] E. Nadal, B. Massuti, M. Dómine, et al., Immunotherapy with checkpoint inhibitors in non-small cell lung cancer: insights from long-term survivors, Cancer Immunol. Immunother. 68 (3) (2019) 341–352.
[12] S.L. Topalian, J.M. Taube, R.A. Anders, D.M. Pardoll, Mechanism-driven biomarkers to guide immune checkpoint blockade in cancer therapy, Nat. Rev. Cancer 16 (5) (2016) 275–287.
[13] R. Cristescu, R. Mogg, M. Ayers, et al., Pan-tumor genomic biomarkers for PD-1 checkpoint blockade-based immunotherapy, Science. 362 (6411) (2018).
[14] R. Liu, F. Yang, J.Y. Yin, et al., Influence of tumor immune infiltration on immune checkpoint inhibitor therapeutic efficacy: a computational retrospective study, Front. Immunol. 12 (2021) 685370.
[15] M. Yi, D. Jiao, H. Xu, et al., Biomarkers for predicting efficacy of PD-1/PD-L1 inhibitors, Mol. Cancer 17 (1) (2018) 129.
[16] H. Rizvi, F. Sanchez-Vega, K. La, et al., Molecular determinants of response to anti-programmed cell death (PD)-1 and anti-programmed death-ligand 1 (PD-L1) blockade in patients with non-small-cell lung cancer profiled with targeted next-generation sequencing, J. Clin. Oncol. : official journal of the American Society of Clinical Oncology 36 (7) (2018) 633–641.
[17] T. Yagi, Y. Baba, T. Ishimoto, et al., PD-L1 Expression, Tumor-Infiltrating Lymphocytes, and Clinical Outcome in Patients with Surgically Resected Esophageal Cancer, vol. 269, 2019, pp. 471–478, 3.
[18] D.J. McGrail, P.G. Pilié, N.U. Rashid, et al., High tumor mutation burden fails to predict immune checkpoint blockade response across all cancer types, Ann. Oncol. 32 (5) (2021) 661–672.
[19] D.P. Carbone, M. Reck, L. Paz-Ares, et al., First-line nivolumab in stage IV or recurrent non-small-cell lung cancer, N. Engl. J. Med. 376 (25) (2017) 2415–2426.
[20] A. Zehir, R. Benayed, R.H. Shah, et al., Mutational landscape of metastatic cancer revealed from prospective clinical sequencing of 10,000 patients, Nat. Med. 23 (6) (2017) 703–713.
[21] W. Zhang, Y. Tang, Y. Guo, et al., Favorable immune checkpoint inhibitor outcome of patients with melanoma and NSCLC harboring FAT1 mutations, npj Precis. Oncol. 6 (1) (2022) 46.
[22] S. Spranger, H.K. Koblish, B. Horton, et al., Mechanism of tumor rejection with doublets of CTLA-4, PD-1/PD-L1, or Ido blockade involves restored IL-2 production and proliferation of CD8+ T cells directly within the tumor microenvironment, Journal for ImmunoTherapy of Cancer. 2 (1) (2014) 3.
[23] S. Bobisse, R. Genolet, A. Roberti, et al., Sensitive and frequent identification of high avidity neo-epitope specific CD8 (+) T cells in immunotherapy-naive ovarian cancer, Nat. Commun. 9 (1) (2018) 1092.
[24] Z. Ou, S. Lin, J. Qiu, et al., Single-nucleus RNA sequencing and spatial transcriptomics reveal the immunological microenvironment of cervical squamous cell carcinoma, Adv. Sci. (2022) e2203040.
[25] J.A. Grout, P. Sirven, A.M. Leader, et al., Spatial positioning and matrix programs of cancer-associated fibroblasts promote T cell exclusion in human lung tumors, Cancer Discov. 12 (11) (2022) 2606–2625.
[26] K. Irshad, C. Srivastava, N. Malik, et al., Upregulation of atypical cadherin FAT1 promotes an immunosuppressive tumor microenvironment via TGF-β, Front. Immunol. 13 (2022) 813888.
[27] A. Lánczky, B. Győrffy, Web-based survival analysis tool tailored for medical research (KMplot): development and implementation, J. Med. Internet Res. 23 (7) (2021) e27633.
[28] Z. Tang, B. Kang, C. Li, T. Chen, Z. Zhang, GEPIA2: an enhanced web server for large-scale expression profiling and interactive analysis, Nucleic Acids Res. 47 (W1) (2019) W556–W560.
[29] J.T. Fekete, B. Győrffy, ROCplot.org: validating predictive biomarkers of chemotherapy/hormonal therapy/anti-HER2 therapy using transcriptomic data of 3,104 breast cancer patients, Int. J. Cancer 145 (11) (2019) 3140–3151.
[30] D. Bu, H. Luo, P. Huo, et al., KOBAS-i: intelligent prioritization and exploratory visualization of biological functions for gene enrichment analysis, Nucleic Acids Res. 49 (W1) (2021) W317–w325.
[31] S. Tian, P. Peng, J. Li, et al., SERPINH1 regulates EMT and gastric cancer metastasis via the Wnt/β-catenin signaling pathway, Aging 12 (4) (2020) 3574–3593.
[32] X. Li, C. Wang, H. Zhang, et al., circFNDC3B accelerates vasculature formation and metastasis in oral squamous cell carcinoma, Cancer Res. 83 (9) (2023) 1459–1475.
[33] D. Zeng, Z. Ye, J. Wu, et al., Macrophage correlates with immunophenotype and predicts anti-PD-L1 response of urothelial cancer, Theranostics 10 (15) (2020) 7002–7014.
[34] Z.G. Chen, N.F. Saba, Y. Teng, The diverse functions of FAT1 in cancer progression: good, bad, or ugly? J. Exp. Clin. Cancer Res. : CR 41 (1) (2022) 248.

[35] X. Hu, Y. Zhai, P. Kong, et al., FAT1 prevents epithelial mesenchymal transition (EMT) via MAPK/ERK signaling pathway in esophageal squamous cell cancer, Cancer Lett. 397 (2017) 83–93.
[36] L. Wang, S. Lyu, S. Wang, et al., Loss of FAT1 during the progression from DCIS to IDC and predict poor clinical outcome in breast cancer, Exp. Mol. Pathol. 100 (1) (2016) 177–183.
[37] S. Lee, S. Stewart, I. Nagtegaal, et al., Differentially expressed genes regulating the progression of ductal carcinoma in situ to invasive breast cancer, Cancer Res. 72 (17) (2012) 4574–4586.
[38] M. Chen, X. Sun, Y. Wang, et al., FAT1 inhibits the proliferation and metastasis of cervical cancer cells by binding β-catenin, Int. J. Clin. Exp. Pathol. 12 (10) (2019) 3807–3818.
[39] G.D. Tran, X.D. Sun, C.C. Abnet, et al., Prospective study of risk factors for esophageal and gastric cancers in the Linxian general population trial cohort in China, Int. J. Cancer 113 (3) (2005) 456–463.
[40] D. Valletta, B. Czech, T. Spruss, et al., Regulation and function of the atypical cadherin FAT1 in hepatocellular carcinoma, Carcinogenesis 35 (6) (2014) 1407–1415.
[41] R.J. DeBerardinis, Tumor microenvironment, metabolism, and immunotherapy, N. Engl. J. Med. 382 (9) (2020) 869–871.
[42] N. Riaz, J.J. Havel, V. Makarov, et al., Tumor and microenvironment evolution during immunotherapy with nivolumab, Cell 171 (4) (2017) 934–949.e916.
[43] S.J. Turley, V. Cremasco, J.L. Astarita, Immunological hallmarks of stromal cells in the tumour microenvironment, Nat. Rev. Immunol. 15 (11) (2015) 669–682.
[44] J.E. Bader, K. Voss, J.C. Rathmell, Targeting metabolism to improve the tumor microenvironment for cancer immunotherapy, Mol. Cell 78 (6) (2020) 1019–1033.
[45] A.M. Newman, C.B. Steen, C.L. Liu, et al., Determining cell type abundance and expression from bulk tissues with digital cytometry, Nat. Biotechnol. 37 (7) (2019) 773–782.
[46] R. Sun, E.J. Limkin, M. Vakalopoulou, et al., A radiomics approach to assess tumour-infiltrating CD8 cells and response to anti-PD-1 or anti-PD-L1 immunotherapy: an imaging biomarker, retrospective multicohort study, Lancet Oncol. 19 (9) (2018) 1180–1191.
[47] K. Ford, C.J. Hanley, M. Mellone, et al., NOX4 inhibition potentiates immunotherapy by overcoming cancer-associated fibroblast-mediated CD8 T-cell exclusion from tumors, Cancer Res. 80 (9) (2020) 1846–1860.
[48] T. Liu, C. Han, S. Wang, et al., Cancer-associated fibroblasts: an emerging target of anti-cancer immunotherapy, J. Hematol. Oncol. 12 (1) (2019) 86.